ChemistrySelect

Research Article
doi.org/10.1002/slct.202201912

Chemistry Europe
European Chemical Societies Publishing

www.chemistryselect.org

A Series of Adenosine Analogs as the First Efficacious Anti-SARS-CoV-2 Drugs against the B.1.1.529.4 Lineage: A Preclinical Repurposing Research Study

Amgad M. Rabie*[a, b] and Mohnad Abdalla*[c]

Given the rapid progression of the coronavirus disease 2019 (COVID-19) pandemic, an ultrafast response was urgently required to handle this major public crisis. To contain the pandemic, investments are required to develop diagnostic tests, prophylactic vaccines, and novel therapies. Lately, nucleoside analog (NA) antivirals topped the scene as top options for the treatment of COVID-19 caused by the severe acute respiratory syndrome coronavirus 2 (SARS-CoV-2) infections. Meanwhile, the continuous generation of new lineages of the SARS-CoV-2 Omicron variant caused a new challenge in the persistent COVID-19 battle. Hitting the two crucial SARS-CoV-2 enzymes RNA-dependent RNA polymerase (RdRp) and 3′-to-5′ exoribonuclease (ExoN) collectively together using only one single ligand is a very successful new approach to stop SARS-CoV-2 multiplication and combat COVID-19 irrespective of the SARS-CoV-2 variant type because RdRps and ExoNs are broadly conserved among all SARS-CoV-2 strains. Herein, the current comprehensive study investigated most NAs libraries, searching for the most ideal drug candidates expectedly able to perfectly act through this double tactic. Gradual computational filtration gave rise to six different promising NAs, which are riboprine, forodesine, tecadenoson, nelarabine, vidarabine, and maribavir, respectively. Further biological assessment proved for the first time, using the *in vitro* anti-RdRp/ExoN and anti-SARS-CoV-2 bioassays, that riboprine and forodesine, among all the six tested NAs, are able to powerfully inhibit the replication of the new virulent strains of SARS-CoV-2 with extremely minute *in vitro* anti-RdRp and anti-SARS-CoV-2 EC_{50} values of about 0.22 and 0.49 μM for riboprine and about 0.25 and 0.73 μM for forodesine, respectively, surpassing both remdesivir and the new anti-COVID-19 drug molnupiravir. The prior *in silico* data supported these biochemical findings, suggesting that riboprine and forodesine molecules strongly hit the key catalytic pockets of the SARS-CoV-2 (Omicron variant) RdRp′s and ExoN′s main active sites. Additionally, the ideal pharmacophoric features of riboprine and forodesine molecules render them typical dual-action inhibitors of SARS-CoV-2 replication and proofreading, with their relatively flexible structures open for diverse types of chemical derivatization. In Brief, the current important results of this comprehensive study revealed the interesting repurposing potentials of, mainly, the two nucleosides riboprine and forodesine to effectively shut down the polymerase/exoribonuclease-RNA nucleotides interactions of the SARS-CoV-2 Omicron variant and consequently treat COVID-19 infections, motivating us to rapidly begin the two drugs′ broad preclinical/clinical anti-COVID-19 bioevaluations, hoping to combine both drugs soon in the COVID-19 treatment protocols.

Introduction

Few months to 2023 and the severe acute respiratory syndrome coronavirus 2 (SARS-CoV-2) is still awfully encircling the globe. Accordingly, our multinational multidisciplinary research team has been in laboratories day and night scrutinizing coronavirus disease 2019 (COVID-19) cases among the different people, aiming to design and develop new therapies against this pathogenic virus, repurpose known medications against the fatal disease, and share our relevant insights and visions with colleagues in Egypt, China, Spain, USA, and other countries. There are some master needs that have yet to be highly or sufficiently met for effective and successful management/treatment of COVID-19 disease.[1–7] In our points of view, the failures (key pitfalls) of many COVID-19 clinical trials can be principally attributed to: (1) actual inefficacies of the examined compounds, specially repurposed ones (i.e., drugs already approved for other diseases, but not primarily developed against COVID-19); (2) inappropriate trial designs; (3) time selection biases, considering the influences of different time trend scenarios, diverse COVID-19 stages, and chronological bias in the treatment effect estimate; (4) population selection biases induced by the selection of individuals, groups, and/or data for analysis with improper randomization and unclear or ineffective exclusion criteria; (5) dose biases due to unclear/imprecise study design characteristics, unplanned dosage changes during the course of the trial,

[a] *Dr. A. M. Rabie*
Dr. Amgad Rabie's Research Lab. for Drug Discovery (DARLD)
Mansoura City 35511, Mansoura, Dakahlia Governorate (Egypt)
E-mail: amgadpharmacist1@yahoo.com
dr.amgadrabie@gmail.com
[b] *Dr. A. M. Rabie*
Head of Drug Discovery & Clinical Research Department
Dikernis General Hospital (DGH)
Magliss El-Madina Street
Dikernis City 35744, Dikernis, Dakahlia Governorate (Egypt)
[c] *Dr. M. Abdalla*
Key Laboratory of Chemical Biology (Ministry of Education)
Department of Pharmaceutics, School of Pharmaceutical Sciences
Cheeloo College of Medicine, Shandong University
44 Cultural West Road, Shandong Province, 250012 (PR China)
E-mail: mohnadabdalla200@gmail.com

and/or ineffective equivalence dosages; (6) variable treatment durations; (7) short follow-up periods; and (8) very low fragility indices, which make the study results less robust in terms of statistical significance.

The difficulty found in proposing new anti-COVID-19 medications arisen from long drug development times and costly endeavors, has meant that COVID-19 research has focused mainly on existing drugs approved or even under investigation for other diseases. Among these repositioned chemicals, only nucleoside analogs (NAs) and polyphenolics (PPhs) have demonstrated significant promising progress as SARS-CoV-2 inhibitors and lytics.[8–19] NAs, specifically, are more promising and highly tolerated.[20] Some nucleoside-like compounds are currently under broad examinations to be comprehensively evaluated as effective candidate anti-COVID-19 drugs, they are either new drugs, e.g., nirmatrelvir and molnupiravir, or repurposed drugs, e.g., remdesivir, GS-441524, GS-443902, cordycepin, didanosine, and favipiravir, with only nirmatrelvir, molnupiravir, and remdesivir being approved for the mild-to-moderate COVID-19 cases.[8–15]

The latest variant of SARS-CoV-2 is the Omicron variant, also known as B.1.1.529 (or BA), first began its tear around the world since about one year, and currently has more than five brothers of lineages, mainly BA.1-BA.5.[21] Omicron variant was arisen from mainly 36 major new mutations in the coronaviral-2 spike (S) proteins of the original Wuhan virus.[22] Targeting the mutation-resistant fixed proteins among all SARS-CoV-2 variants, e.g., replication RNA-dependent RNA polymerase (RdRp) and proofreading 3′-to-5′ exoribonuclease (ExoN) enzymes, through repurposing approved or under-investigation drugs is a very effective and time-saving approach in the therapeutic COVID-19 battle, even against the expectedly coming resistant SARS-CoV-2 strains. Drugs targeting the replication/proofreading enzymes have unbounded number of incessant opportunities to struggle the coronavirus and its successors, hindering their further multiplication throughout the entire human body (even if these remedies were taken after the incidence of the infection). In the first months of 2022, we as a multinational research team continued our scientific journey and worked around the clock to discover effective, potent, and safe anti-SARS-CoV-2-Omicron-variant drug candidates.

On the other hand, tactical nucleoside analogism is one of the most favorable therapeutic selections in drug designers′ minds to stop the coronavirus reproduction inside the human body.[9–15,20] In this therapeutic tactic against COVID-19 the used nucleoside/nucleotide analog makes use of its close likeness with the genuine biological nucleosides and nucleotides to delude and mislead the SARS-CoV-2 RdRp (the nonstructural protein complex 12/7/8 or nsp12-nsp7-nsp8) and ExoN (the nonstructural protein complex 14/10 or nsp14-nsp10) enzymes.[20] Nsp12-nsp7-nsp8 and nsp14-nsp10 protein complexes are very essential enzymes in the replication/proofreading processes of the coronaviral-2 genome, and, therefore, their significant inhibition will strongly block the proliferation of SARS-CoV-2 particles. Nucleoside-like agents confuse the RdRp and ExoN enzymes through perfect incorporation in the viral genetic RNA strands instead of the correct naturally-occurring nucleosides/nucleotides, leading to excessive repeated ambiguous coding and premature termination of RNA generation with the formation of vague RNA strands at the end; these faulty strands represent almost abnormal, non-infectious, and inactive particles, so there would not be any further multiplication of the coronavirus.[13,14,20] Some of the aforementioned anti-COVID-19 agents, e.g., remdesivir and molnupiravir alongside their active metabolites, GS-441524 and β-D-N^4-hydroxycytidine (NHC), respectively (Figure 1A), primarily depend on this highly effective antiviral mechanism in their inhibitory and/or blocking actions on the SARS-CoV-2 particles.[9–12] With the accelerating emergence of more resistant new species of SARS-CoV-2, finding more effective and broad-spectrum anti-SARS-CoV-2 drugs (natural or synthetic) became an exigency.

In the present work, we have scouted the binary inhibitory activities of some NAs on both SARS-CoV-2 RdRp and ExoN enzymes as a novel effective strategy to dually combat COVID-19.[23] After sieving of several libraries of nucleosides/NAs, we chose the top fifteen nucleoside-like compounds with the best results to establish a very small library for our work (Figure 1B). Almost all the fifteen finalist NAs were adenosine analogs. *In silico* molecular docking revealed that mainly six of these fifteen compounds showed very good binding energies with the two targeted enzymes, SARS-CoV-2 RdRp and ExoN, when compared to binding energies of the two standard drugs (references), remdesivir/molnupiravir, with the same two targeted enzymes. However, the other compounds of the fifteen ones, such as neplanocin A, tubercidin, and cladribine, displayed comparatively moderate-to-good outcomes. Molecular docking and dynamics simulations studies of the opted six compounds disclosed the relative superiority of the two nucleosidic compounds riboprine and forodesine in hitting the catalytic active sites of both targeted enzymes with the formation of more stable complexes of higher negative binding energies. Similarly, biological evaluation of the six NAs against both coronaviral-2 RdRp and ExoN proteins and against the entire SARS-CoV-2 Omicron variant particles showed nearly the same promising superiority of riboprine and forodesine, respectively.

Depending on the current research findings supported with the previous results,[24–27] we can conclude that, first, riboprine and forodesine can be further *in vivo* and clinically tested for repurposing potential against COVID-19 and, second, the foreseeable significant clinical inhibitory actions of riboprine and forodesine against SARS-CoV-2 replication may be primarily attributed to the ternary synergistic inhibitory activities against the three pivotal enzymes RdRp, ExoN, and adenosine kinase (ADK), i.e., closely related to the RdRp, ExoN, and ADK inhibitory activities of riboprine/forodesine. The possible SARS-CoV-2 RNA mutagenicity of both NAs *via* nucleoside analogism mode of action and inclusion into the new coronaviral-2 RNA strands should also be adequately and clinically studied. In addition, the pharmacokinetics of these nucleosidic drugs should be considerably put into account, because different cellular/tissue distributions of these prospective anti-SARS-CoV-2 agents will undoubtedly affect their gross capabilities of

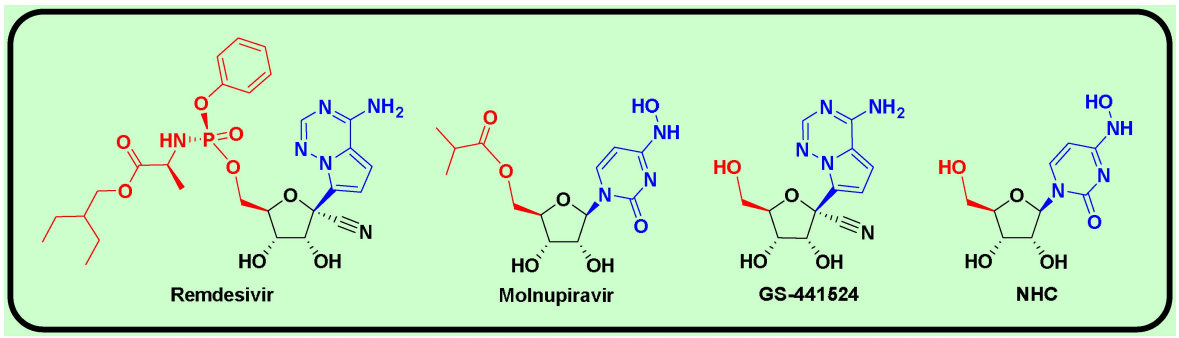

A

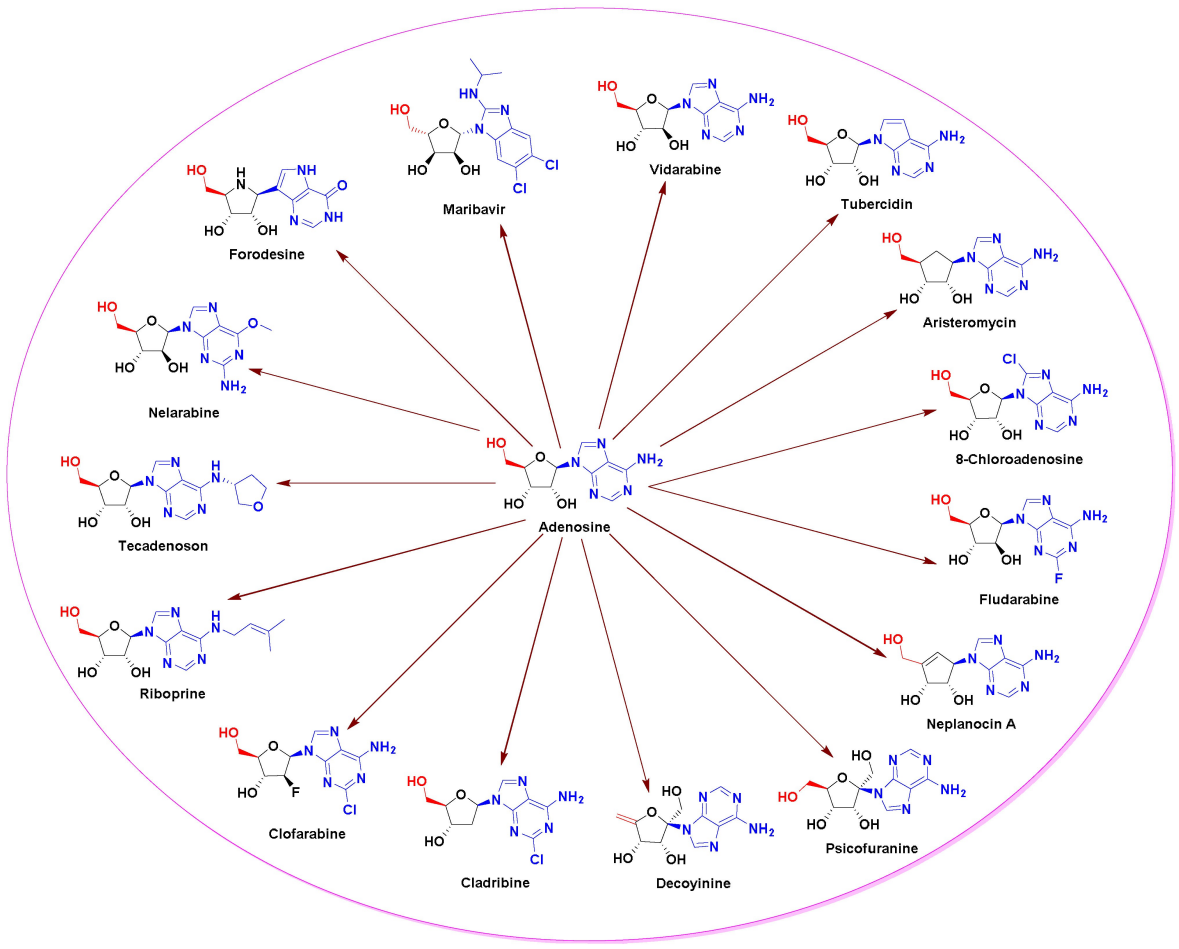

B

Figure 1. Chemical structures of: **A**) Reference anti-SARS-CoV-2 drugs, remdesivir and molnupiravir and their active metabolites, GS-441524 and NHC, respectively. **B**) Adenosine and its explored fifteen analogs as potential anti-SARS-CoV-2 drugs.

reducing the viral loads of SARS-CoV-2 in COVID-19 therapy.[28] The possibility of medicinally formulating the successful anti-SARS-CoV-2 nucleoside-like agents, among the six tested ones, as fast-action oral/nasal anti-COVID-19 drops/spray should also be properly considered.

Materials and Methods

In silico computational evaluation methodology

Preparation of targeted coronaviral-2 enzymes

The 3D molecular structures of the targeted SARS-CoV-2 RdRp and ExoN proteins were obtained from the RCSB Protein Data Bank (PDB) with PDB identification codes (IDs) 7BV2 and 7MC6,

respectively. Both enzymatic proteins were obtained in the complex forms with their protein cofactors (i.e., were obtained cocrystallized in the nsp12-nsp7-nsp8 and nsp14-nsp10 complex forms, respectively) to increase nature simulation. The PDB files of the two proteins were properly downloaded. Proteins were viewed through Pymol Molecular Graphic Visualizer software 2.4, and their prerecognized active site residues (with their closest surrounding residues) were then inspected for full existence/rightness. The catalytic active pocket residues highlighted *via* Pymol software were noted for the next *in silico* studies.

Selection/preparation of nucleosidic ligands

To pick out the ideal NAs for the current study, a preliminary virtual screening of various libraries of hundreds of NAs was carried out against the SARS-CoV-2 RdRp and ExoN proteins, employing the Molecular Operating Environment (MOE) platform (Chemical Computing Group) for this purpose. The fifteen NAs with the best collective findings (i.e., the best hitting ligands for the two targeted enzymes) were chosen to continue the long journey of this current research work. Following this accurate screening, a thorough literature check was also done searching for any expectancies and prospects of the chosen fifteen NAs to be antivirals. Many of them have displayed significant antiviral capacities either in biological or *in silico* studies or, sometimes, in both of them. This is actually one of the principal causes for trying these possible inhibitors in the present advanced virtual docking/simulation studies against the SARS-CoV-2 RdRp/ExoN proteins. The chemical structures of the chosen fifteen NAs were adequately outfitted (for all the planned *in silico* studies) utilizing a licensed version of ChemDraw software (Version Professional 16.0).

Molecular docking protocol

Undirected docking of the fifteen selected NAs in SARS-CoV-2 RdRp and ExoN proteins was performed *via* MOE. Remdesivir (with the hydroxyls of its phosphate moiety being in the free form in order to be matched with the tested NAs) and molnupiravir were used as positive control anti-SARS-CoV-2 references due to their proven potent RdRp/ExoN inhibitory activities. Prior to starting these docking procedures, some necessary preparations (e.g., additions and corrections) were required. All the missed atoms/residues in the SARS-CoV-2 RdRp and ExoN were added *via* MOE structure modeling. The two targeted enzymatic proteins, RdRp/ExoN, were precisely prepared for molecular docking by the addition of hydrogen atoms using the 3D-protonation module of the employed MOE software; any partial charges were also properly corrected for both proteins. RdRp and ExoN enzymes (in their complex forms) were energy minimized using the Amber-99 force field which is available in MOE. Similarly, the structures of the fifteen target ligands and the two reference ligands (remdesivir/molnupiravir) were also adequately energy minimized in MOE. For docking of the target/reference ligands with the two proteins, the known London-dG scoring functions were utilized for accurate binding energy calculations. For each docked NA/reference molecule, the MOE software generated about twenty different poses with each docked SARS-CoV-2 enzyme. Of all the docking poses for each molecule with each protein, the one with the highest number of best molecular interactions, i.e., the best pose or the top ranked interactions, was scored and saved. MOE gives a numeric value for the interaction of any candidate ligand with any particular protein in the form of a docking S-score (docking scores are expressed in kcal/mol). This docking binding energy/S-score represents the net energy of the created protein-ligand complex and it also reflects the degree of its expected stability in principle (i.e., it provides a first idea about the foretold stability of this formed complex before making the more detailed robust computations *via* the molecular dynamics "MD" simulation process). The *in silico* docking showed mainly six promising target NAs with very good to excellent S-scores as compared to the two reference NAs (these top ranked NAs represent the core point of the present research work). MOE software displays all the probable molecular interactions (of all types) made during the docking process. These molecular interactions include hydrogen bonding (H-bonds), hydrophobic interactions, ionic interactions/bonds, salt bridges, and others. For the best six target NAs and the two reference NAs, the 2D and 3D output images of all the generated protein-ligand complexes (demonstrating nearly all the possible interactions) were saved for scientific publication later and further computational analyses.

Molecular dynamics (MD) simulation protocol

The six NAs ranked with the top results, e.g., with the best molecular interactions, highest negative docking score (S-score), and lowest root-mean-square deviation (RMSD), estimated *via* MOE against both proteins (using the relevant apoenzyme for comparison in each case) were also selected for further *in silico* studies (mainly the thorough MD simulation studies), employing Schrodinger's Desmond module MD-Simulation software with its specific parameters and force fields. For MD simulation of the selected NAs, the best docking poses of these NAs in complexes with the SARS-CoV-2 RdRp and ExoN enzymes were kept in PDB format in MOE to be used for further virtual stability studies in Schrodinger's Desmond module. The in-built Desmond System Builder tool was used in this current protocol to create the solvated water-soaked MD-Simulation system. The TIP3P model was utilized as the solvating model in the present experiment. With periodic boundary conditions, an orthorhombic box was accurately simulated with a good boundary distance of at least 10 Å from the outer surface of each of the two coronaviral-2 proteins. The simulation systems were neutralized of complex charges by the addition of a reasonably sufficient amount of counter ions. The isosmotic state was maintained by adding 0.10 mol/L sodium and chloride ions, i.e., 0.10 M NaCl, into the simulation panel. Prior to beginning the current simulation process, a predefined equilibration procedure was done. The system of the MD simulation was equilibrated by employing the standard Desmond protocol at a fixed pressure of nearly 1.0 bar and a

fixed temperature of 300 K (NPT ensemble; considering the microbial origin of the targeted proteins), and also by employing the validated Berendsen coupling protocol with one temperature group. H-bond length was duly constrained using the known SHAKE algorithm. Particle Mesh Ewald (PME) summation method was used to particularly pattern long-range electrostatic interactions. On the other side, a rigorous cutoff of exactly 10 Å was specially assigned for van der Waals and short-range electrostatic interactions. As aforementioned, the MD simulation was run at ambient pressure conditions of 1.013 bar while the used temperature was precisely set to 300 K for each 100 nsec (ns) period of this MD simulation, and about 1000 frames were saved into the simulation trajectory file. The simulation run times for all complex systems and aposystems were exactly fixed to be 100 ns in each time. After the concurrent and successive simulations, trajectory files of the simulated systems were successfully employed for computation and estimation of the several studied structural parameters, for instance, RMSD (Å), root-mean-square fluctuation (RMSF; Å), radius of gyration (rGyr; Å), number of protein-ligand contacts (# of total contacts), interactions fractions (%), intermolecular H-bonds (from all aspects), molecular surface area (MolSA; $Å^2$), solvent-accessible surface area (SASA; $Å^2$), and polar surface area (PSA; $Å^2$), to comprehensively implement and fulfill the *in silico* stability studies of the complex systems and aposystems. The outcomes of the top promising two NAs, riboprine and forodesine, were stored to be adequately reported and discussed in the present article.

In vitro biological evaluation methodology

Specifications of the bioexamined NAs

Riboprine (N^6-(2-Isopentenyl)adenosine, CAS Registry Number: 7724-76-7) was purchased from BenchChem (BENCH CHEMICAL, Austin, Texas, U.S.A.) (Catalog Number: B141774, Purity: $\geq$99%). While forodesine (Immucillin-H, CAS Registry Number: 209799-67-7), nelarabine (Arranon, CAS Registry Number: 121032-29-9), tecadenoson (CVT-510, CAS Registry Number: 204512-90-3), maribavir (1263W94, CAS Registry Number: 176161-24-3), vidarabine (Arabinosyladenine "Ara-A", CAS Registry Number: 5536-17-4), remdesivir (GS-5734, CAS Registry Number: 1809249-37-3), and molnupiravir (EIDD-2801, CAS Registry Number: 2349386-89-4) were purchased from Biosynth Carbosynth (Carbosynth Ltd., Berkshire, U.K.) (for forodesine, Product Code: MD11591, Purity: $\geq$98%; for nelarabine, Product Code: NN26176, Purity: $\geq$98%; for tecadenoson, Product Code: EIA51290, Purity: $\geq$98%; for maribavir, Product Code: AM178224, Purity: $\geq$98%; for vidarabine, Product Code: NA06007, Purity: $\geq$98%; for remdesivir, Product Code: AG170167, Purity: $\geq$98%; for molnupiravir, Product Code: AE176721, Purity: $\geq$98%). The ultrapure solvent dimethylsulfoxide (DMSO, CAS Registry Number: 67-68-5) was purchased from a local distributor, El-Gomhouria Company For Drugs (El-Gomhouria Co. For Trading Drugs, Chemicals & Medical Supplies, Mansoura Branch, Egypt) (Purity: $\geq$99.9% "anhydrous").

In vitro anti-RdRp/anti-ExoN assay (SARS-CoV-2-RdRp-Gluc Reporter Assay) of the selected NAs

At the beginning, the used cells, 293T cells (ATCC CRL-3216), were kept in Dulbecco's modified Eagle's medium (DMEM; Gibco) with 10% (v/v) fetal bovine serum (FBS; Gibco), then they were cultured at 37 °C in a humidified atmosphere of CO_2 (5%). HEK293T cells were transfected using Vigofect transfection reagents (Vigorous) according to the proper instructions of the manufacturer. The prerequisite plasmid DNAs/antibodies/reagents were bought and handled exactly as in the literature procedures.[24,25] The assayed drugs are as characterized in the previous subsection. Also, western blotting (for the collected transfected HEK293T cells), real-time RT-PCR (for the extracted total RNA of transfected HEK293T cells), and cell viability test (using Cell Counting Kit-8 (CCK8), Beyotime) were exactly performed as the typical procedures of the literature.[24,25] The steps of the well-designed *in vitro* SARS-CoV-2-RdRp-Gluc Reporter Assay were accurately carried out according to the same authentic method of literature but with almost all the proteins being modified to be relevant to the SARS-CoV-2 Omicron subvariant "B.1.1.529/BA.4 lineage" (HEK293T cells were transfected in this biochemical assay with CoV-Gluc, nsp12, nsp7, and nsp8 plasmid DNAs at the ratio of 1:10:30:30, and with CoV-Gluc, nsp12, nsp7, nsp8, nsp10, and nsp14 plasmid DNAs at the ratio of 1:10:30:30:10:90).[24,25] Similarly as instructed in the genuine assay, a stock of coelenterazine-h was dissolved in very pure absolute ethanol to an exact concentration of 1.022 mM.[24,25] Immediately prior to each assay, the stock was diluted in phosphate-buffered saline (PBS) to a concentration of approximately 16.7 μM and incubated in the dark for 30 min at room temperature.[24,25] For luminescence assay, 10 μL of the supernatant was added to each well of a white and opaque 96-well plate, then 60 μL of 16.7 μM coelenterazine-h was injected, followed by measurement of the luminescence for 0.5 s using the Berthold Centro XS3 LB 960 microplate luminometer.[24,25] Final results were statistically represented as the mean (μ) $\pm$ the standard deviation (*SD*) from at least three independent experiments. Statistical analysis was performed using SkanIt 4.0 Research Edition software (Thermo Fisher Scientific) and Prism V5 software (GraphPad). All the resultant data were considered statistically significant at $p < 0.05$.

In vitro anti-SARS-CoV-2 and cytotoxic bioactivities multiassay of the selected NAs

This validated *in vitro* anti-COVID-19 multiassay (including the cytotoxicity test), which was designed for the assessment of the net anti-SARS-CoV-2 activities of candidate anti-COVID-19 agents, is chiefly dependent upon the authentic procedures of Rabie.[5,13,14,16–19] The steps of this multiassay were entirely carried out in an authorized specific biosafety level 3 (BSL-3) laboratory. The assayed new strain of SARS-CoV-2 virus, the Omicron subvariant, B.1.1.529/BA.4 lineage, was isolated from the fresh nasopharynx aspirate and throat swab of a 39.5-year-old Spanish man with confirmed COVID-19 infection using Vero

E6 cells (ATCC CRL-1586) on 8 May, 2022. The starting titer of the stock virus ($10^{7.25}$ $TCID_{50}$/mL) was prepared after three serial passages in Vero E6 cells in infection media (DMEM supplemented with 4.5 g/L D-glucose, 100 mg/L sodium pyruvate, 2% FBS, 100000 U/L Penicillin-Streptomycin, and 25 mM *N*-(2-hydroxyethyl)piperazine-*N*′-ethanesulfonic acid (HEPES)). The examined target/reference NAs are as previously described. Preliminary pilot assays were performed mainly to set the ideal concentration of all the tested NAs to begin the *in vitro* anti-SARS-CoV-2 and cytotoxicity tests with. Accordingly, the stocks of the tested NAs were precisely prepared by dissolving each of the eight compounds in DMSO to obtain a 100 μM concentration of each compound. Furthermore, DMSO was employed for the purpose of a negative control comparator to render this experimental study placebo-controlled. To evaluate the overall *in vitro* anti-SARS-CoV-2 activity of each of the target drugs, riboprine, forodesine, nelarabine, tecadenoson, maribavir, and vidarabine, in comparison to that of each of the two positive control/reference drugs, remdesivir and molnupiravir, along with that of the negative control solvent, DMSO, Vero E6 cells were pretreated with each of the nine compounds diluted in infection media for 1 h prior to infection by the new Omicron variant of the SARS-CoV-2 virus at MOI = 0.02. The nine tested compounds were maintained with the virus inoculum during the 2-h incubation period. The inoculum was removed after incubation, and the cells were overlaid with infection media containing the diluted test compounds. After 48 h of incubation at 37 °C, supernatants were directly collected to quantify viral loads by $TCID_{50}$ assay or quantitative real-time RT-PCR "qRT-PCR" (TaqMan Fast Virus 1-Step Master Mix). Viral loads in this assay were fitted in logarithm scale (log_{10} $TCID_{50}$/mL, log_{10} $TCID_{90}$/mL, and log_{10} viral RNA copies/mL), not in linear scale, under increasing concentrations of the tested compounds. Four-parameter logistic (4PL) regression (GraphPad Prism) was utilized to properly fit the dose-response curves and determine the EC_{50} and EC_{90} of the tested compounds that inhibit SARS-CoV-2 viral replication ($CPEIC_{100}$ was also determined for each compound). In addition, cytotoxicity of each of the nine tested compounds was also evaluated in Vero E6 cells using the CellTiter-Glo Luminescent Cell Viability Assay (Promega). Final results were statistically represented as the $\mu \pm SD$ from at least three independent experiments. Statistical analysis was done using SkanIt 4.0 Research Edition software (Thermo Fisher Scientific) and Prism V5 software (GraphPad). All the resultant data were considered statistically significant at $p < 0.05$.

Results and Discussion

Computational molecular modeling of the selected NAs as potential anti-COVID-19 drugs

After computational screening and filtration of several libraries of nucleosides and NAs as previously discussed in the methodology, the top fifteen nucleoside-like molecules with the best and most ideal pharmacodynamic/pharmacokinetic findings with respect to the prospective anti-SARS-CoV-2 properties were chosen for our specific mission. The opted compounds were as follows: riboprine, forodesine, tecadenoson, nelarabine, vidarabine, maribavir, neplanocin A, tubercidin, cladribine, decoyinine, aristeromycin, fludarabine, clofarabine, psicofuranine, and 8-chloroadenosine, respectively. Consequently, a very small and specific new library was established of these aforementioned fifteen natural/synthetic compounds (Figure 1B). In a next step, further molecular docking specifically against SARS-CoV-2 RdRp and ExoN disclosed that the compounds riboprine, forodesine, tecadenoson, nelarabine, vidarabine, and maribavir, respectively, have the lowest and best binding energies (ranged from −6.8 to −8.2 kcal/mol) compared to the two reference anti-RdRp/anti-ExoN drugs, remdesivir and molnupiravir (having binding energies ranged from −6.6 to −7.5 kcal/mol), as shown in Table 1. The catalytic pockets (i.e., active sites) of the two SARS-CoV-2 enzymes, RdRp (which is the main enzyme responsible for replication and transcription of the SARS-CoV-2 RNA genome) and ExoN (this proofreading nsp14 or exoribonuclease of SARS-CoV-2 has two main active pockets; the exoribonuclease active site, the one that we are concerned with in the present work, and the methyltransferase active site), were almost defined and validated *via* several previous computational, crystallographic, and biochemical studies in the literature.[29–32] Exploring and analyzing the resultant *in silico* interactions of the above-mentioned six molecules with the amino acids of SARS-CoV-2 RdRp and ExoN proteins demonstrated that all these molecules considerably strike most residues of the catalytic pockets of the two enzymes with strong interactions, including, mainly, H-bonds, hydrophobic interactions, ionic bonds, and water bridges (less strong in some examples), of comparatively short bond distances and low binding energies.

Table 1. The binding affinity energy values (docking S-scores) estimated during molecular docking of the fifteen screened NAs against the two SARS-CoV-2 proteins, RdRp and ExoN enzymes (using remdesivir and molnupiravir as the positive control drugs). The fifteen NAs are arranged in a collective descending order, beginning from the top ranked one and ending with the least ranked one.

Compound	Classification	Docking S-score [kcal/mol]	
		RdRp (7BV2)	ExoN (7MC6)
Screened NAs	Riboprine	−7.5	−8.2
	Forodesine	−7.7	−7.9
	Tecadenoson	−7.4	−7.8
	Nelarabine	−7.5	−7.3
	Vidarabine	−7.3	−7.2
	Maribavir	−6.8	−7.5
	Neplanocin A	−7.2	−6.9
	Tubercidin	−7.0	−6.7
	Cladribine	−6.9	−6.7
	Decoyinine	−6.3	−7.1
	Aristeromycin	−6.2	−7.1
	Fludarabine	−6.2	−6.9
	Clofarabine	−6.2	−6.8
	Psicofuranine	−6.1	−6.8
	8-Chloroadenosine	−6.0	−6.6
Reference Drugs	Remdesivir	−6.8	−7.4
	Molnupiravir	−6.6	−7.5

Figures 2A,**B** and **3A**,**B** demonstrate, respectively, the itemized 2D/3D representations of the most evident intermolecular interactions between each ligand of the six ones with each of the two coronaviral-2 enzymes/proteins. The 3D representations mostly focus on the shortest bonds. The molecules of these six NAs strongly hit most neighboring active residues of the major catalytic pocket of SARS-CoV-2 RdRp (in chain A, i.e., 7BV2-A receptor), e.g., Arg553, Arg555, Thr556, Ala558, Lys621, Cys622, Asp623, Arg624, Thr680, Ser681, Ser682, Thr687, Ala688, Asn691, Leu758, Ser759, Asp760, Asp761, and Cys813. On the other side, the molecules of the same six NAs powerfully strike most of the adjacent active residues of the major catalytic pocket (exoribonuclease active site) of SARS-CoV-2 ExoN (in chain A; QHD43415_13 receptor), e.g., Asp90, Val91, Glu92, Gly93, Cys94, His95, Asn104, Pro141, Phe146, Leu149, Trp186, Ala187, Gly189, Phe190, Gln191, Asn252, Leu253, Gln254, His268, and Asp273. These interactions are very promising and very comparable to, or even in many cases considerably better than, those of remdesivir and molnupiravir with the same proteins.

Analysis of the MD simulation results revealed the relative considerable stabilities of the formed protein-ligand complexes of each of the six NAs with each of the two enzymes when compared with the reference drugs. Complexes of the NAs with SARS-CoV-2 ExoN are slightly more stable, with less numbers/intensities of fluctuations, and with lower RMSD (Å) and RMSF (Å) values than those with SARS-CoV-2 RdRp. Interestingly, riboprine and forodesine displayed the best results among all in most of the compared MD items during the simulation. Comprehensively, the RdRp-riboprine, RdRp-forodesine, ExoN-riboprine, and ExoN-forodesine complexes appear to be stable with acceptable degrees. The early fluctuations (which, mostly, were not extreme) in RMSF and RMSD trajectories may be indications of some conformational changes within the enzyme complex system due to adequate repositioning of both ligands inside the catalytic binding pockets, which takes some nanotime, till the formation of interesting vigorous molecular interactions. Undisclosed conceivable allosteric modulations, specially in case of the larger protein complex SARS-CoV-2 nsp12-nsp7-nsp8, could also be put into consideration. Forodesine has the lowest rGyr values (less than 3.5 Å) among all the tested compounds, including the references, with both enzymes, indicating more compact and stable protein systems. In addition, from the computational point of view, forodesine followed by riboprine have the best balanced MolSA, SASA, and PSA values among all the investigated compounds. Interestingly, riboprine displayed the largest interactions fraction (of more than 2% of the total interactions predicted) of the strong H-bonds with the hit SARS-CoV-2 proteins, among all the tested compounds, and this occurs specifically with the catalytic amino acid residue Asp90 in the small protein SARS-CoV-2 nsp14-nsp10 in its relatively stable complex with riboprine, indicating a significant potential of riboprine to allow a strongly-inhibited/blocked status of the ExoN enzyme. MD simulation results also confirmed nearly all the primary molecular docking data with regard to, for example, the interacting amino acids along with the numbers/types/strengths of the formed bonds. Exhaustively, Figure 4A,B, Figure 5A,B, Figure 6A,B, Figure 7A,B, and Figure 8A,B show the detailed results of MD simulation of the interactions between each ligand of the most promising NAs, riboprine and forodesine, with each of the two coronaviral-2 enzymes, RdRp and ExoN, respectively (in comparison with the two reference FDA-approved anti-SARS-CoV-2 RdRp drugs, remdesivir and molnupiravir). The previous computational data were very motivating to persuade us to transfer to the biological assessment part of the current research.

Experimental biological evaluation of the selected NAs as potential anti-COVID-19 drugs

The direct biochemical enzyme assay in this extensive assessment is the *in vitro* cell-based anti-SARS-CoV-2 RdRp test, which was lately developed in the last two years through using Gaussia-luciferase (Gluc) as the reporter to estimate the anticoronaviral-2 RdRp activity of principally the NAs (the prodrugs of nucleotides) without any obligatory necessity for producing or obtaining the active nucleotidic triphosphate forms of the NAs (or of the other nontriphosphorylated nucleotidic analogs, i.e., of the monophosphorylated and diphosphorylated NAs), unlike the situation in the cell-free assays.[24,25] In addition, it was confirmed without a doubt, through the findings of this new robust assay, that the exonuclease activity of SARS-CoV-2 nsp14 significantly improves the SARS-CoV-2 RdRp resistance to the various therapeutic inhibitors of the nucleoside/nucleotide analog class (one of the primary factors that aggravates the resistance and severe pathogenicity of SARS-CoV-2 virus is its ability to encode the nsp14 ExoN which is competent of tearing out the faulty mutagenic nucleotides misincorporated by the low-fidelity RdRp into the growing coronaviral-2 RNA strands, resulting in significant resistance to antiviral agents of the nucleoside/nucleotide analog type), thus these relevant ExoN capabilities were considered and properly assessed in the procedure of this screening assay protocol which was primarily planned and designed for exploring possible SARS-CoV-2 RdRp inhibitors (dissimilar to the traditional analytical cell-free assay).[24,25,33,34] The assay can be also generally called "antireplicative activity bioassay".

As mentioned earlier, we focus at most in the present work on the two principal protein complexes that catalyze and regulate the pivotal SARS-CoV-2 replication/transcription bioprocesses, nsp12-nsp7-nsp8 polymerase complex and nsp14-nsp10 exoribonuclease complex, respectively. This reporter test significantly mimics the SARS-CoV-2 RNA generating processes which are induced and controlled majorly by the RdRp enzyme.[35] Table 2 displays the detailed values obtained from this *in vitro* anti-SARS-CoV-2 RdRp/ExoN bioassay. The resultant data showed that the two NAs riboprine and forodesine demonstrated the best outcomes among all. The two compounds effectively suppressed SARS-CoV-2 RdRp activity with very excellent small EC_{50} values of 0.22 and 0.25 μM, which very slightly increased in the presence of SARS-CoV-2 ExoN (the wild

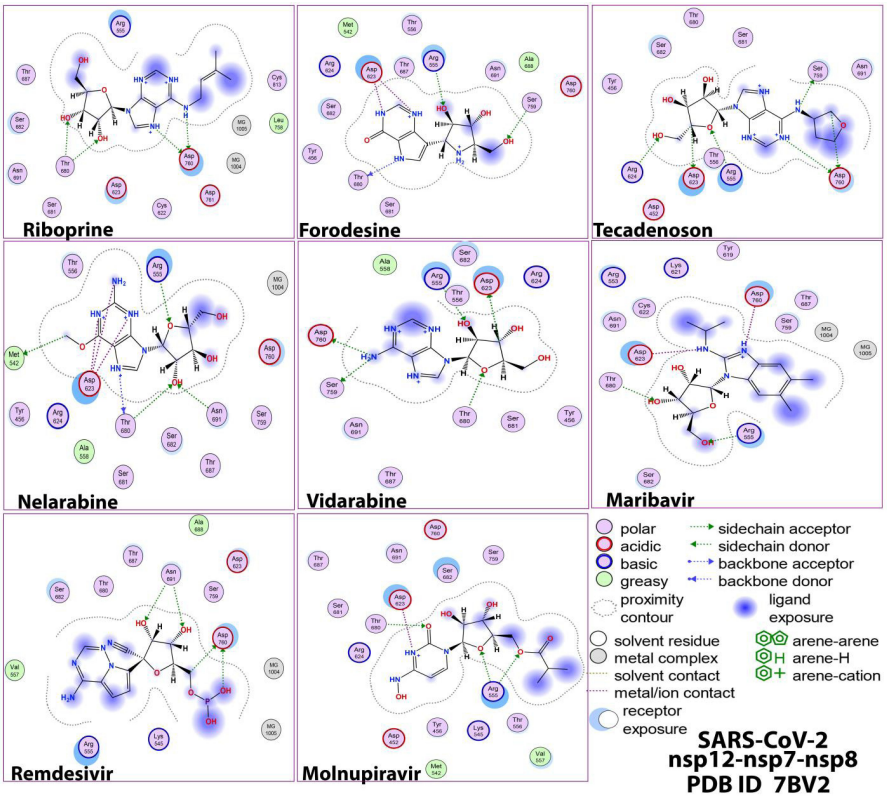

A

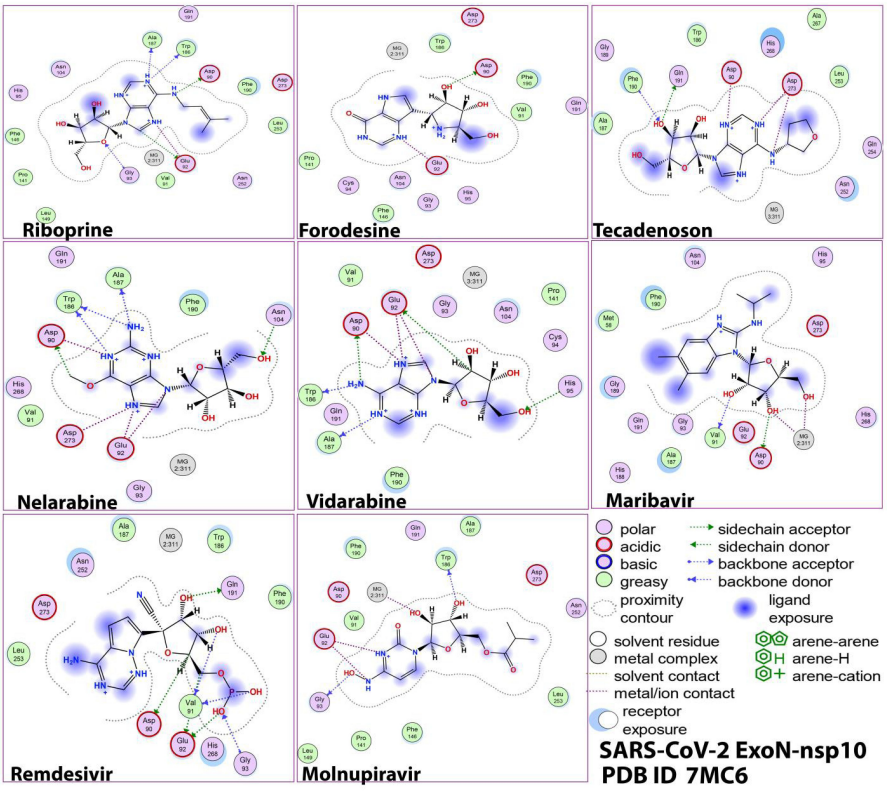

B

Figure 2. 2D images of the postdocking interactions of the six NAs, riboprine, forodesine, tecadenoson, nelarabine, vidarabine, and maribavir, and the two reference drugs, remdesivir and molnupiravir, respectively, with: (**A**) SARS-CoV-2 RdRp "nsp12" enzyme cocrystallized with its protein cofactors nsp7 and nsp8 (PDB ID: 7BV2). (**B**) SARS-CoV-2 ExoN "nsp14" enzyme cocrystallized with its protein cofactor nsp10 (PDB ID: 7MC6).

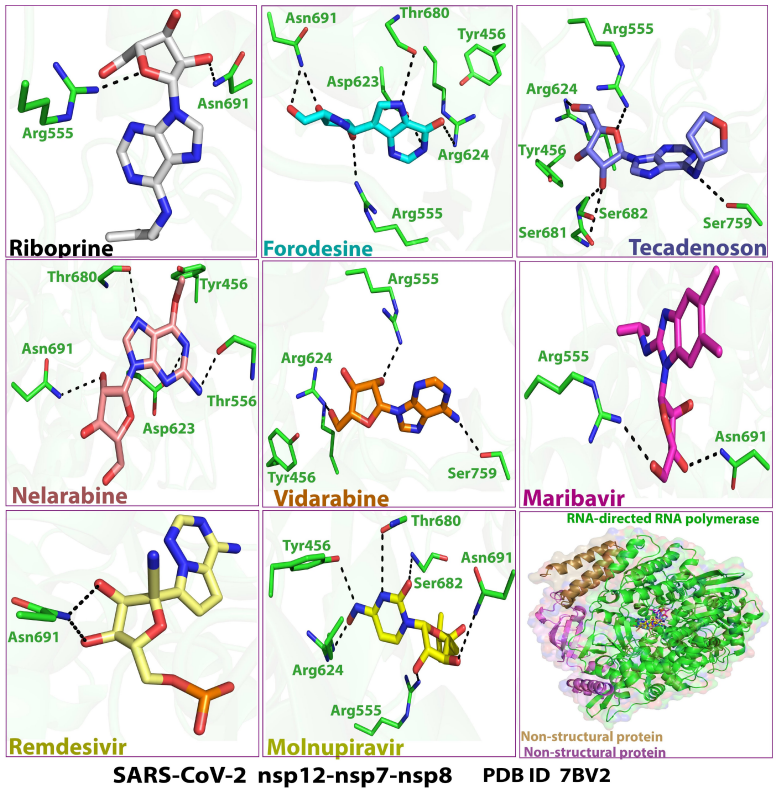

A

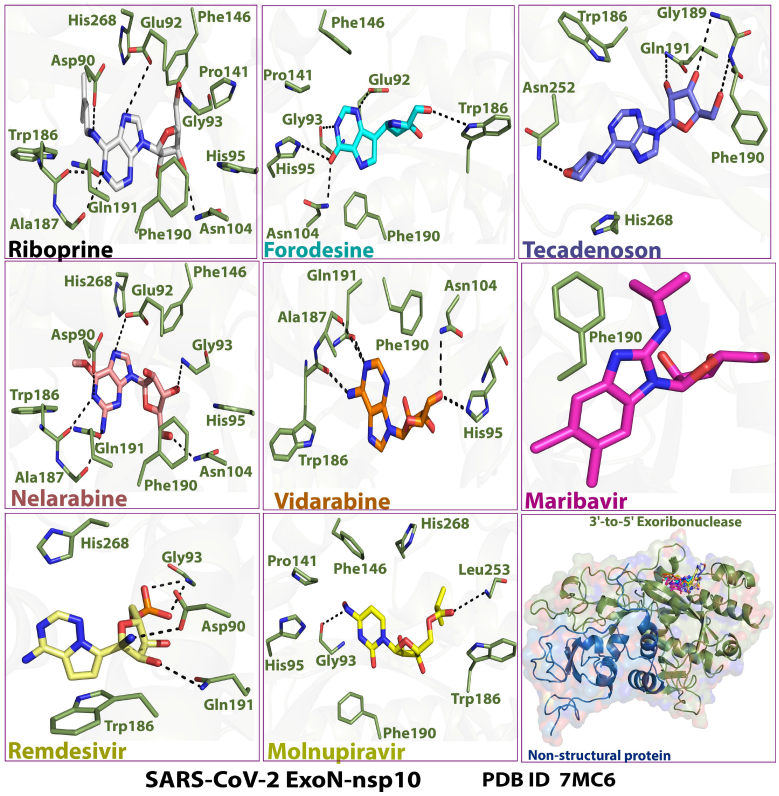

B

Figure 3. 3D images of the postdocking interactions of the six NAs, riboprine, forodesine, tecadenoson, nelarabine, vidarabine, and maribavir, and the two reference drugs, remdesivir and molnupiravir, respectively, with: (**A**) SARS-CoV-2 RdRp "nsp12" enzyme cocrystallized with its protein cofactors nsp7 and nsp8 (PDB ID: 7BV2). (**B**) SARS-CoV-2 ExoN "nsp14" enzyme cocrystallized with its protein cofactor nsp10 (PDB ID: 7MC6).

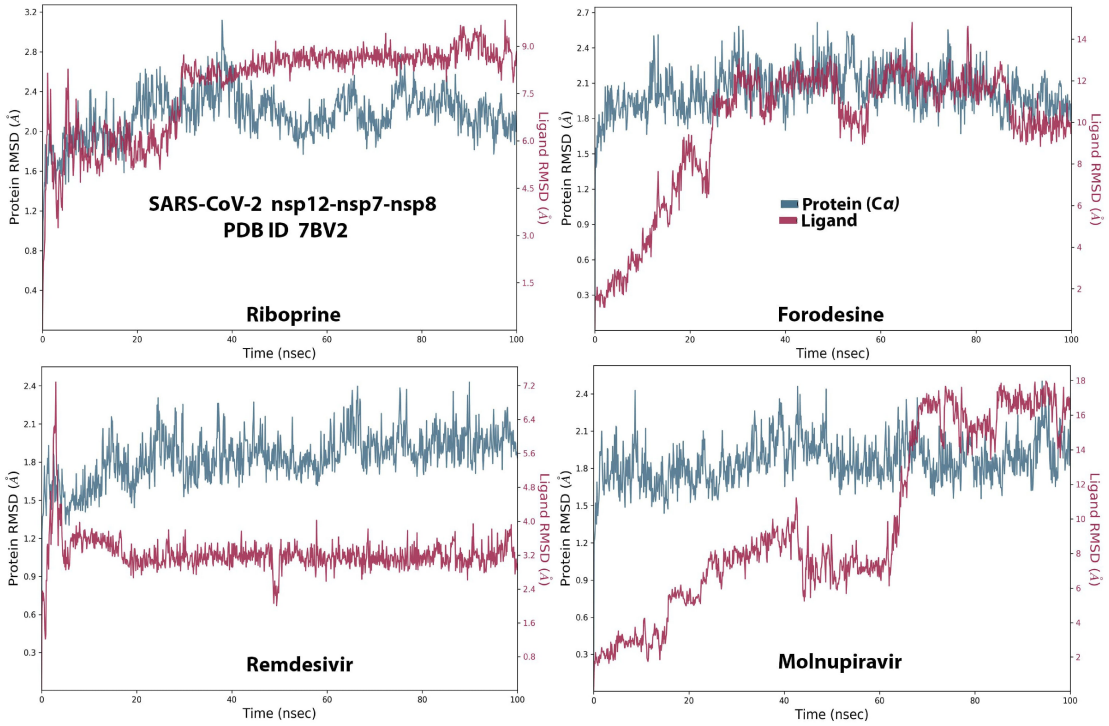

A

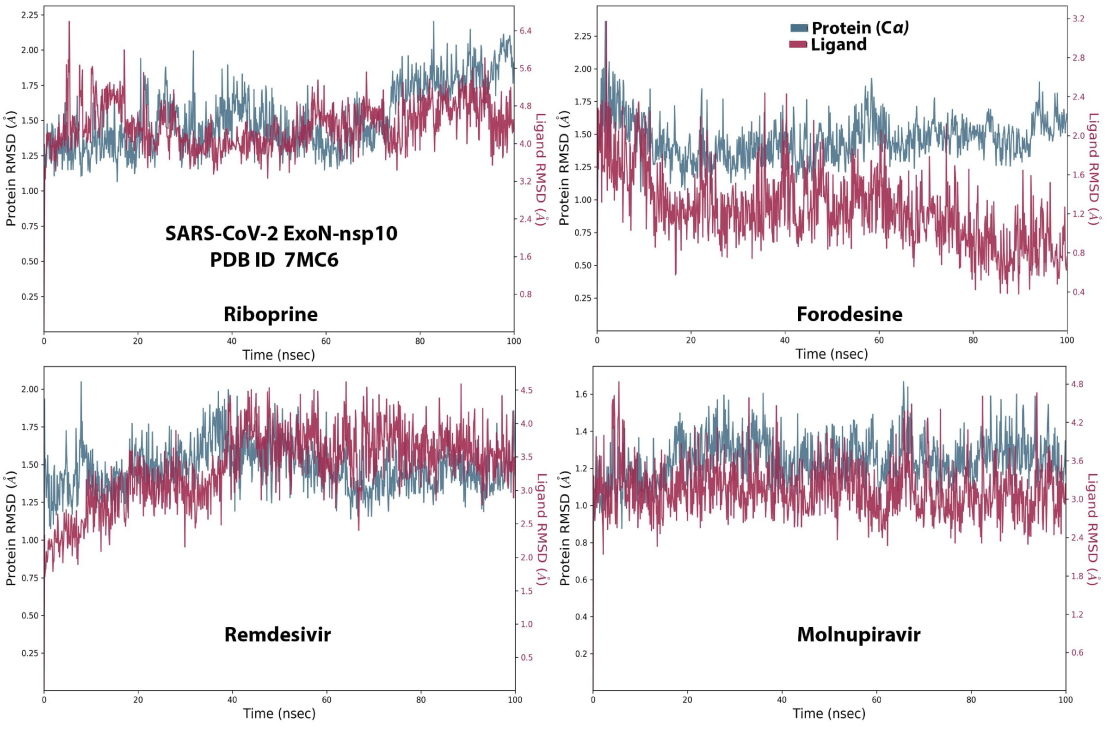

B

Figure 4. RMSD trajectories (during a simulation period of 100 ns) of the α-carbon of amino acid residues of the protein (blue color) and the ligand (maroon color) in the protein-ligand complexes of the two NAs, riboprine and forodesine, and the two reference drugs, remdesivir and molnupiravir, respectively, with: (**A**) SARS-CoV-2 RdRp "nsp12" enzyme cocrystallized with its protein cofactors nsp7 and nsp8 (PDB ID: 7BV2). (**B**) SARS-CoV-2 ExoN "nsp14" enzyme cocrystallized with its protein cofactor nsp10 (PDB ID: 7MC6).

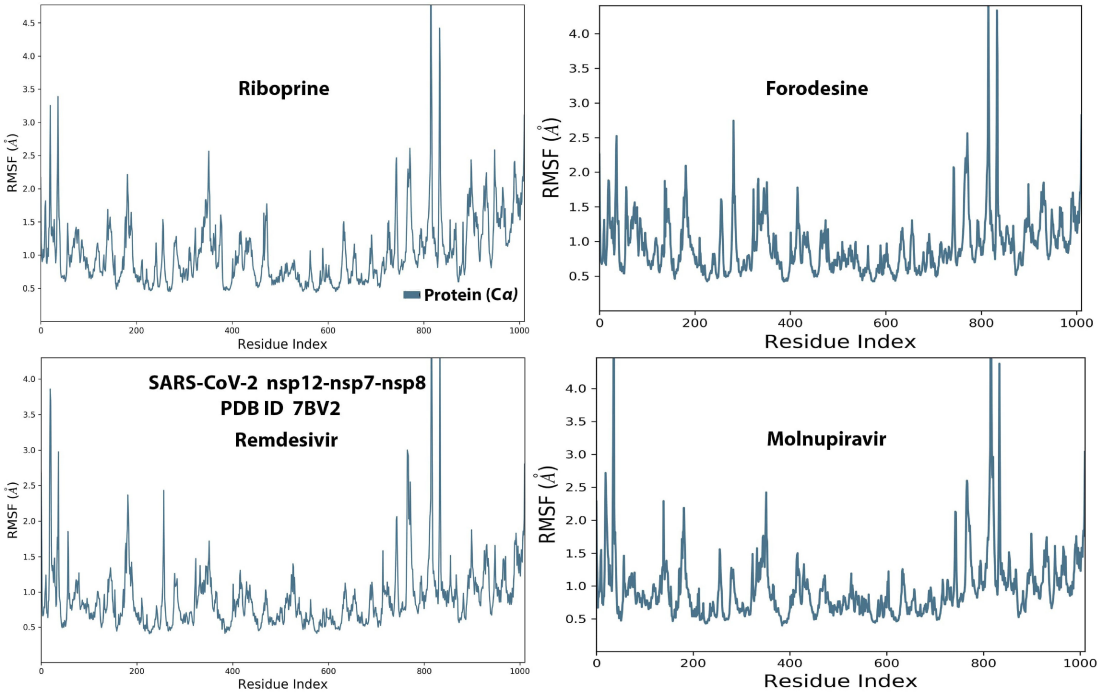

Figure 5. RMSF trajectories (along the different residue regions) of the α-carbon of amino acid residues of the protein in the protein-ligand complexes of the two NAs, riboprine and forodesine, and the two reference drugs, remdesivir and molnupiravir, respectively, with: (**A**) SARS-CoV-2 RdRp "nsp12" enzyme cocrystallized with its protein cofactors nsp7 and nsp8 (PDB ID: 7BV2). (**B**) SARS-CoV-2 ExoN "nsp14" enzyme cocrystallized with its protein cofactor nsp10 (PDB ID: 7MC6).

type) to about 0.33 and 0.35 μM, respectively, indicating the potent inhibitory/blocking activities of both compounds against SARS-CoV-2 ExoN, which appeared in these extremely minute nanomolar differences of the EC_{50} values between the two conditions. Modifications in the exoribonuclease structure (i.e., the mutated type; e.g., D90A/E92A mutations of the

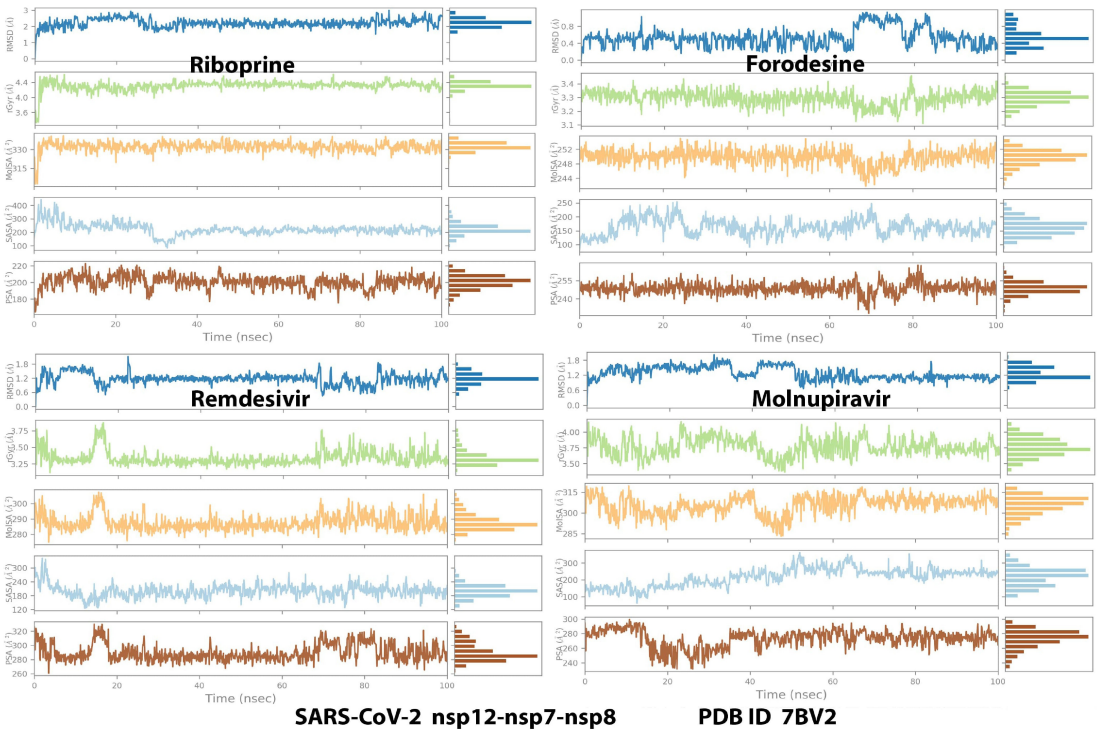

Figure 6. Collective post-MD simulation analysis of the protein-ligand complexes properties (RMSD, rGyr, MolSA, SASA, and PSA) of the two NAs, riboprine and forodesine, and the two reference drugs, remdesivir and molnupiravir, respectively, with: (**A**) SARS-CoV-2 RdRp "nsp12" enzyme cocrystallized with its protein cofactors nsp7 and nsp8 (PDB ID: 7BV2). (**B**) SARS-CoV-2 ExoN "nsp14" enzyme cocrystallized with its protein cofactor nsp10 (PDB ID: 7MC6).

amino acid sequence of active site in nsp14 as in our current case) reinforced the anti-RdRp activity of riboprine and forodesine to excellent EC_{50} values of 0.27 and 0.30 μM (i.e., slightly lower than that resulted in the presence of the normal

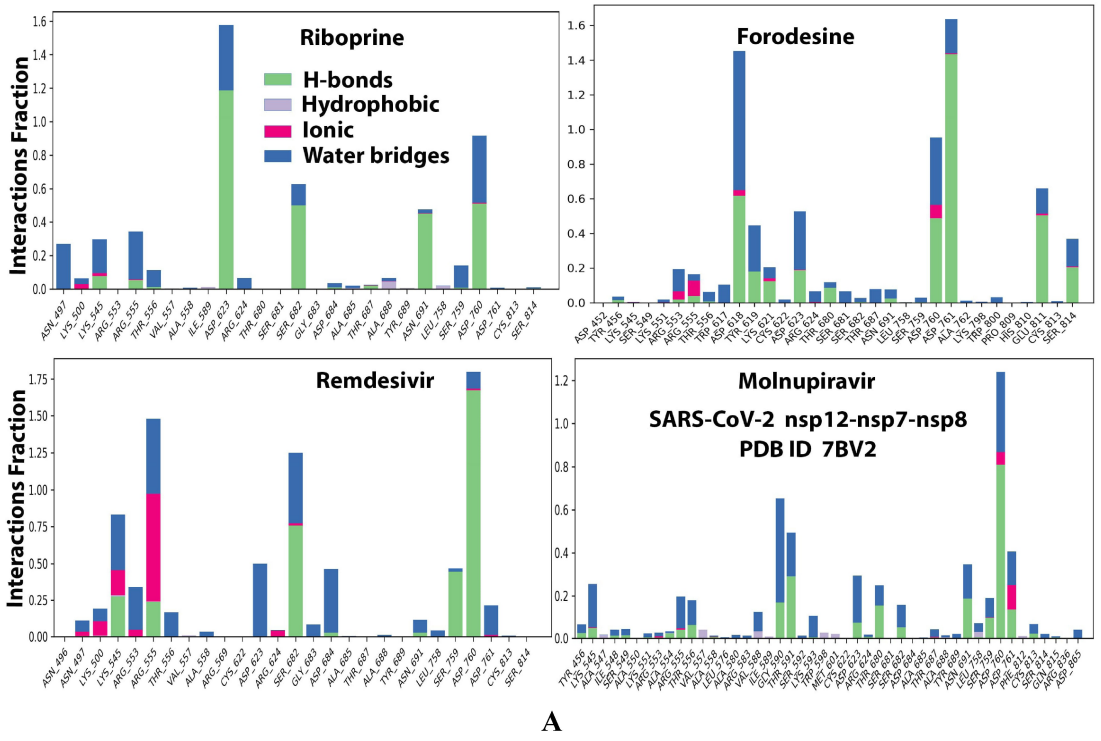

A

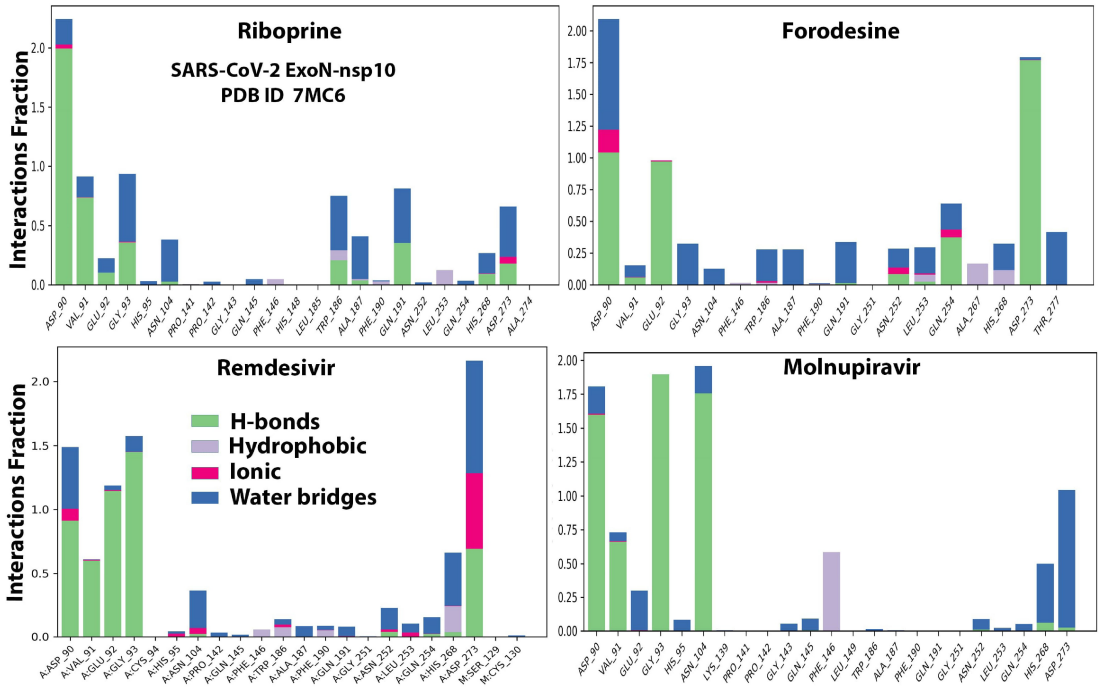

B

Figure 7. Histograms of the protein-ligand interactions fractions throughout the simulative interaction trajectories of the two NAs, riboprine and forodesine, and the two reference drugs, remdesivir and molnupiravir, respectively, with: (**A**) SARS-CoV-2 RdRp "nsp12" enzyme cocrystallized with its protein cofactors nsp7 and nsp8 (PDB ID: 7BV2). (**B**) SARS-CoV-2 ExoN "nsp14" enzyme cocrystallized with its protein cofactor nsp10 (PDB ID: 7MC6).

wild type of ExoN; these very slight changes also reflected, as aforementioned, the potent activities of both NAs against SARS-CoV-2 ExoN in its original wild type from the beginning before examining any induced mutations). These previous values of riboprine and forodesine even clearly surpassed those of the two potent standard medicines, remdesivir/molnupiravir, which showed higher values, reflecting the prospective preponderance of both NAs over remdesivir and molnupiravir

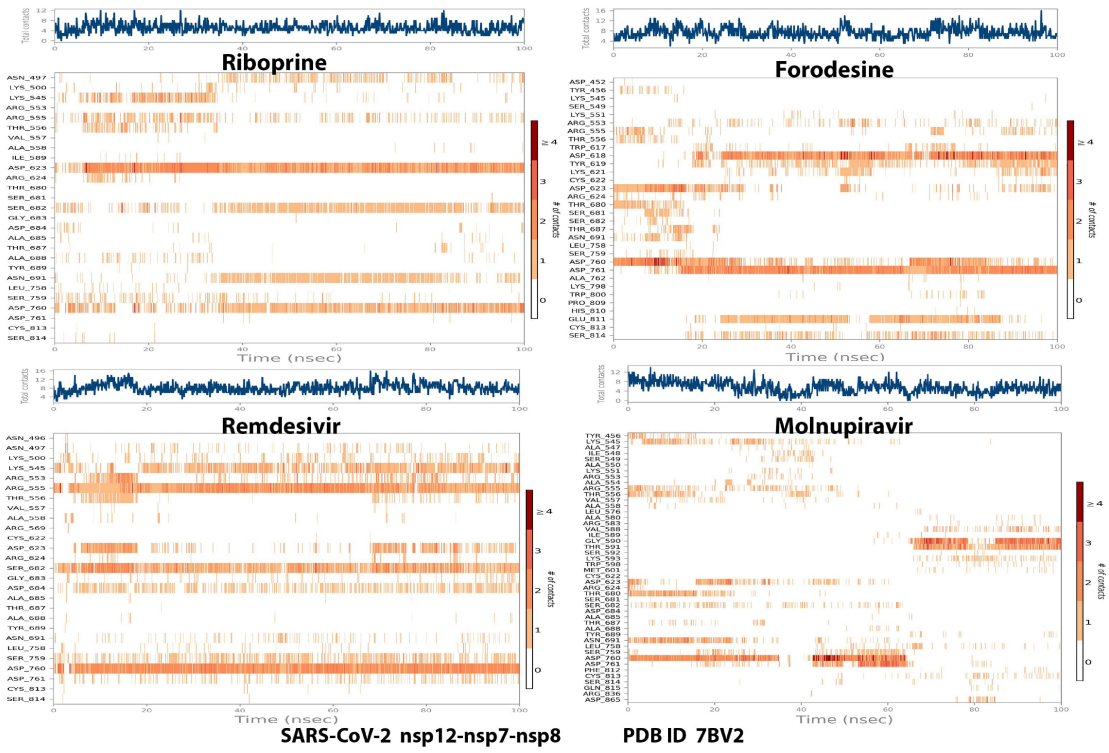

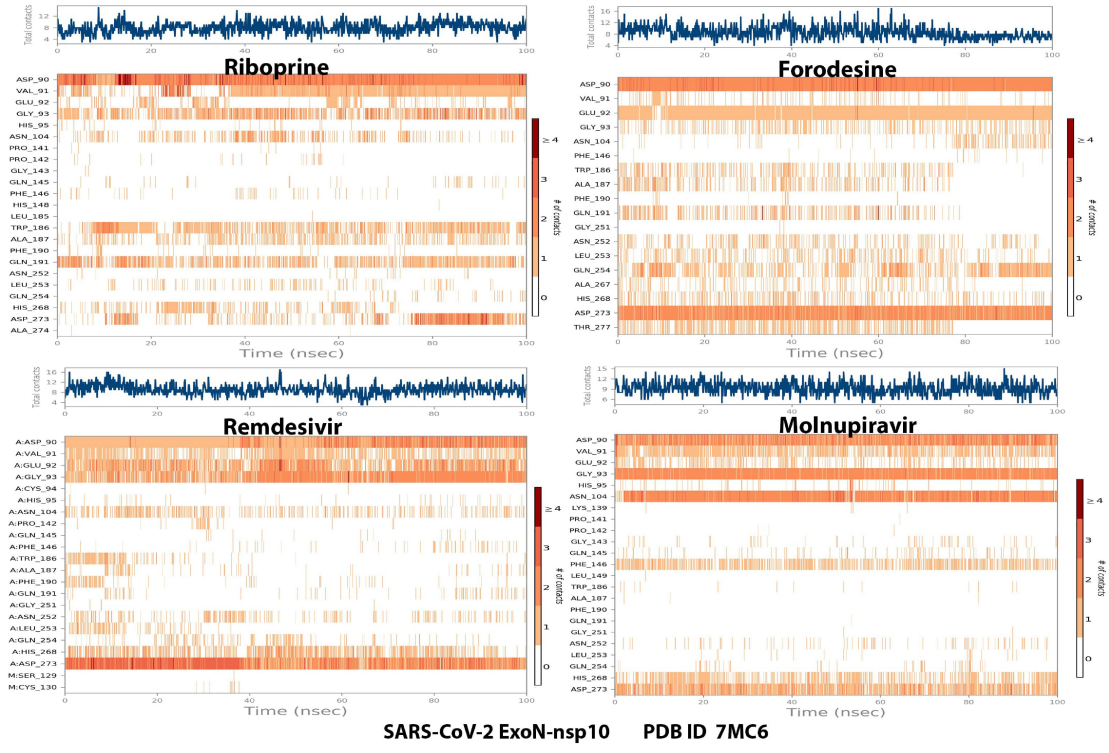

Figure 8. Plots of the distribution of the total number of interactions (contacts) in each trajectory framework of the protein-ligand complexes of the two NAs, riboprine and forodesine, and the two reference drugs, remdesivir and molnupiravir, respectively, with: (**A**) SARS-CoV-2 RdRp "nsp12" enzyme cocrystallized with its protein cofactors nsp7 and nsp8 (PDB ID: 7BV2). (**B**) SARS-CoV-2 ExoN "nsp14" enzyme cocrystallized with its protein cofactor nsp10 (PDB ID: 7MC6).

Table 2. Anti-SARS-CoV-2 RdRp/ExoN activities (along with the respective ratios) of the six target drugs in HEK293T cells. Remdesivir and molnupiravir were used as the positive control/reference drugs, and DMSO as the negative control/placebo drug.

Classification	Compound	EC_{50} [μM][a] Nsp12	Nsp12 + Nsp14	Nsp12 + $Nsp14_{mutant}$	EC_{50} Ratio (Nsp12 + Nsp14)/Nsp12	(Nsp12 + $Nsp14_{mutant}$)/Nsp12
Repurposed NAs	Riboprine	0.22 ± 0.03	0.33 ± 0.04	0.27 ± 0.03	1.50	1.23
	Forodesine	0.25 ± 0.03	0.35 ± 0.04	0.30 ± 0.04	1.40	1.20
	Nelarabine	0.69 ± 0.05	1.25 ± 0.07	1.15 ± 0.06	1.81	1.67
	Tecadenoson	1.05 ± 0.06	1.42 ± 0.08	1.34 ± 0.08	1.35	1.28
	Maribavir	1.11 ± 0.06	1.95 ± 0.09	1.56 ± 0.07	1.76	1.41
	Vidarabine	1.15 ± 0.07	2.10 ± 0.09	1.59 ± 0.08	1.83	1.38
Reference Drugs	Remdesivir	1.20 ± 0.08	2.19 ± 0.10	1.64 ± 0.08	1.83	1.37
	Molnupiravir	0.29 ± 0.04	0.50 ± 0.05	0.39 ± 0.05	1.72	1.35
Placebo Solvent	DMSO	> 100	> 100	> 100	N.A.[b]	N.A.

[a] Test compound concentration required for 50% decrease in SARS-CoV-2 RdRp activity *in vitro;* Nsp12 refers to nsp12/7/8 complex, Nsp14 refers to nsp14/10 complex, and $Nsp14_{mutant}$ refers to $nsp14_{mutant}$/10 complex. [b] N.A.: not available (i.e., not determined).

in clinical use in humans (if applicable). The findings also demonstrated that molnupiravir and remdesivir could not resist the actions of Omicron variant ExoN enzyme the same leverage riboprine and forodesine do. The other four target NAs, nelarabine, tecadenoson, maribavir, and vidarabine, also exhibited good promising and small values, but with less degrees than those of riboprine, forodesine, and the positive control molnupiravir, respectively. It is apparently observed from the values in Table 2 that as much the EC_{50} values of the NA against the polymerase alone and against the polymerase in the presence of the exoribonuclease are close to each other, as more predicted for this tested NA to be an ideally effective SARS-CoV-2 RdRp/replication inhibitor. The very interesting biological capabilities of riboprine and forodesine to hinder and inhibit the nsp12 polymerase/nsp14 exoribonuclease activities of the coronaviral-2 Omicron variant promisingly boost the repurposing potentials of riboprine and forodesine in clinical settings for further medicinal usage as effective and powerful anti-COVID-19 drugs. These existing biochemical results concerning the very potent inhibitory SARS-CoV-2 RdRp-binding and ExoN-binding characteristics of riboprine and forodesine are in a very acceptable agreement with most estimated items of the previously-discussed *in silico* part of the present work.

The latter assay is collectively the *in vitro* anti-SARS-CoV-2/cytotoxicity tests. Table 3 presents the resultant values from the two tests in details. The used SARS-CoV-2 strain in this collective assay is the new variant of SARS-CoV-2, the Omicron

Table 3. Anti-SARS-CoV-2/anti-COVID-19 activities (along with cytotoxicities) of the six target drugs. Remdesivir and molnupiravir were used as the positive control/reference drugs, and DMSO as the negative control/placebo drug against SARS-CoV-2 (Omicron subvariant, B.1.1.529/BA.4 lineage) in Vero E6 cells.

Classification	Compound	CC_{50} [μM][a]	Inhibition of SARS-CoV-2 Replication *in vitro* (Anti-B.1.1.529/BA.4 Bioactivities) [μM]			
			100% CPE Inhibitory Concentration ($CPEIC_{100}$)[b]	50% Reduction in Infectious Virus (EC_{50})[c]	50% Reduction in Viral RNA Copy (EC_{50})[d]	90% Reduction in Infectious Virus (EC_{90})[e]
Repurposed NAs	Riboprine	> 100	1.23 ± 0.05	0.49 ± 0.03	0.50 ± 0.03	1.69 ± 0.08
	Forodesine	> 100	1.71 ± 0.08	0.73 ± 0.04	0.75 ± 0.04	2.31 ± 0.09
	Nelarabine	> 100	4.37 ± 0.17	1.75 ± 0.07	1.81 ± 0.08	6.66 ± 0.20
	Tecadenoson	> 100	7.87 ± 0.24	2.93 ± 0.11	2.97 ± 0.12	11.95 ± 0.29
	Maribavir	> 100	8.22 ± 0.25	3.09 ± 0.11	3.21 ± 0.13	12.68 ± 0.30
	Vidarabine	> 100	8.31 ± 0.25	3.28 ± 0.12	3.33 ± 0.12	13.01 ± 0.32
Reference Drugs	Remdesivir	> 100	6.06 ± 0.19	2.09 ± 0.08	2.15 ± 0.08	8.30 ± 0.26
	Molnupiravir	> 100	6.50 ± 0.22	2.72 ± 0.10	2.80 ± 0.09	9.98 ± 0.28
Placebo Solvent	DMSO	> 100	> 100	> 100	> 100	> 100

[a] CC_{50} or 50% cytotoxic concentration is the concentration of the tested compound that kills half the cells in an uninfected cell culture. CC_{50} was determined with serially-diluted compounds in Vero E6 cells at 48 h postincubation using CellTiter-Glo Luminescent Cell Viability Assay (Promega). [b] $CPEIC_{100}$ or 100% CPE inhibitory concentration is the lowest concentration of the tested compound that causes 100% inhibition of the cytopathic effects (CPE) of SARS-CoV-2 B.1.1.529/BA.4 virus in Vero E6 cells under increasing concentrations of the tested compound at 48 h postinfection. Compounds were serially diluted from 100 μM concentration. [c] EC_{50} or 50% effective concentration is the concentration of the tested compound that is required for 50% reduction in infectious SARS-CoV-2 B.1.1.529/BA.4 virus particles *in vitro.* EC_{50} is determined by infectious virus yield in culture supernatant at 48 h postinfection (log_{10} $TCID_{50}$/mL). [d] EC_{50} or 50% effective concentration is the concentration of the tested compound that is required for 50% reduction in SARS-CoV-2 B.1.1.529/BA.4 viral RNA copies *in vitro.* EC_{50} is determined by viral RNA copies number in culture supernatant at 48 h postinfection (log_{10} RNA copies/mL). [e] EC_{90} or 90% effective concentration is the concentration of the tested compound that is required for 90% reduction in infectious SARS-CoV-2 B.1.1.529/BA.4 virus particles *in vitro.* EC_{90} is determined by infectious virus yield in culture supernatant at 48 h postinfection (log_{10} $TCID_{90}$/mL).

subvariant B.1.1.529/BA.4 lineage, which is one of the newest infectious and resistant lineages of the virus. The demonstrated data in the table interestingly uncovered the significantly higher antiviral efficacies of each of the two NAs riboprine and forodesine against the newly-emerged variants of SARS-CoV-2 as compared to those of each of the two standard drugs remdesivir and molnupiravir (the negative control placebo solvent, DMSO, exhibited extremely weak activities, i.e., almost negligible results). Riboprine and forodesine were found to actively hinder and block the entire SARS-CoV-2 multiplication in the employed Vero E6 cells with EC_{50} values extremely smaller than the stock concentration value (100 μM), keeping their preponderances over the other tested target NAs exactly as in the preceding biochemical anti-RdRp/ExoN assay. The natural NA riboprine was found to be promisingly leading (i.e., classified as the best inhibitor among all the tested nucleosidic ligands) in its total anti-Omicron-BA.4 activity ($EC_{50} = 0.49$ μM), which was found to be about 4.3 and 5.6 times as effective as the two reference drugs remdesivir ($EC_{50} = 2.09$ μM) and molnupiravir ($EC_{50} = 2.72$ μM), respectively, with respect to the tested *in vitro* anti-B.1.1.529/BA.4/anti-SARS-CoV-2 activity. While forodesine was ranked second, among all the tested nucleosidic ligands, in its total anti-Omicron-BA.4 activity ($EC_{50} = 0.73$ μM), which was found to be about 2.9 and 3.7 times as effective as the two reference drugs remdesivir and molnupiravir, respectively, with respect to the same anti-B.1.1.529/BA.4/anti-SARS-CoV-2 activity. According to the present cytotoxicity assay, the *in vitro* CC_{50} values of riboprine and forodesine are adequately higher than 100 μM, subsequently these two NAs are predicted to have salutary high corresponding clinical selectivity indices "SIs" ($SI_{riboprine} > 204.1$ and $SI_{forodesine} > 137$; while remdesivir and molnupiravir have narrower SIs, $SI_{remdesivir} > 47.9$ and $SI_{molnupiravir} > 36.8$), reflecting the highly selective anti-RNA activities of the riboprine/forodesine molecules against the genome of the Omicron virus rather than that of the human. Similarly, riboprine and forodesine demonstrated very small values of the concentration that leads to 100% reduction in the coronaviral-2 Omicron variant cytopathic effects ($CPEIC_{100} = 1.23$ and 1.71 μM, respectively), which are less than the corresponding values of remdesivir ($CPEIC_{100} = 6.06$ μM) and molnupiravir ($CPEIC_{100} = 6.50$ μM) and also less than those of the other tested NAs. In harmony with their significantly potent activities against the pathogenic coronaviral-2 B.1.1.529/BA.4 strain, riboprine/forodesine also exhibited very slight values of the concentration that is needed for 50% decrease in the number of RNA copies of the B.1.1.529/BA.4 strain of SARS-CoV-2 (0.50 and 0.75 μM, respectively), which are apparently lower than the corresponding values of both remdesivir/molnupiravir (2.15 and 2.80 μM, respectively). EC_{90} values for riboprine and forodesine were also small and in agreement with the EC_{50} values (they were not that much far from the EC_{50} values, indicating the prospective significant clinical potencies of both drugs) as demonstrated in Table 3. The four remaining NAs, Nelarabine, tecadenoson, maribavir, and vidarabine, presented slightly higher concentration values (EC_{50}, EC_{90}, CC_{50}, and $CPEIC_{100}$) than those shown by riboprine/forodesine, but still significantly comparable to those of the two standard drugs.

Another important and favorable observation noted in the present anti-SARS-CoV-2 assay is the comparatively rapid mode of antiviral action (which reaches its peak after 5–9 h of administration) of the two NAs riboprine and forodesine against the Omicron-BA.4 lineage particles. Identical to their natural analogs, the triphosphate esters of riboprine and forodesine (riboprine-TP and forodesine-TP), which are *in vivo* identified as the major metabolic phosphorylated forms of the two molecules, are expected to be as efficient and potent as the administered original basic forms or even slightly more (due to the significantly high biocompatibility). The present outcomes of this validated bioassay are in a very good compliance with almost all the results of the prior anti-RdRp assay and the computational study (which was discussed in details in the prior subsection) of this current comprehensive study.

It is also noteworthy that the anti-DNA, anti-RNA, antimetabolic, and cytotoxic activities of the nucleoside/nucleotide-like compounds riboprine/riboprine-TP and forodesine/forodesine-TP may give rise to some related side effects upon clinical use in humans. The potentials to cause these adverse effects increase in special patient populations, such as children, pregnant/lactating women, the elderly, and hepatic-disease patients, therefore the behaviors and dosages of the currently-explored NAs should be additionally and carefully studied in these groups of population with much attention to evaluate the clinical safety of these potential anti-COVID-19 drugs.

Conclusions

Antiviral nucleosidic agents are nowadays considered as the first available and offered options for COVID-19 remediation.[36] The current dual *in silico*/*in vitro* study disclosed the considerable anti-COVID-19 potentials of a series of NAs, with riboprine and forodesine being the most favorable potent SARS-CoV-2 RNA deactivators or, at least, the most favorable coronaviral-2 replication spoilers in general among the whole series. Riboprine is a natural phytochemical purine nucleoside analog investigated for its many potential pharmacological actions, such as the antineoplastic/antiproliferative, antiangiogenic, proapoptotic, and neuroprotective activities,[37] while forodesine is an approved, very potent, unrivaled, synthetic, and highly selective transition-state analog inhibitor of the known purine nucleoside phosphorylase (PNP), employed for the effective treatment of relapsed/refractory peripheral T-cell lymphoma in the recent years.[38] Physicochemically, riboprine and forodesine have very flexible molecular structures that can adequately tolerate chemical modulations in living systems. It was clearly demonstrated in the existing research work that coronaviral-2 Omicron particles are highly sensitive to both NAs and extensively mutated by them. These actions fundamentally occur through impairing and blocking SARS-CoV-2 replication *via* a binary synergistic inhibitory mode of action against the two vital SARS-CoV-2 proteins RdRp and ExoN. This double mode of anticoronaviral-2 action might be expanded to

be a triple mode if the probable inhibitory actions of the two drugs against kinases, specially on ADK, are extensively studied and confirmed in a next work. Like their natural analogs, the triphosphate forms of riboprine/forodesine are predicted to be as effective as the administered original forms. This present research is part of a series of studies, we have recently done, for exploring the actions of several NAs on different lineages of the SARS-CoV-2 Omicron variant, with the computational section being partly fixed in these studies.[39,40] Based on the current research observations, the two NAs, riboprine and forodesine, are specifically prioritized as prospective anti-COVID-19 therapeutic drugs (with very promising anti-SARS-CoV-2 EC_{50} values of 0.49 and 0.73 μM, respectively, against the pathogenic SARS-CoV-2 Omicron variant), while all the currently-investigated NAs (the entire explored NAs series in the present study), in general, warrant further pharmacological and clinical studies in order to adequately understand and explain their exact therapeutic significances as candidate anti-SARS-CoV-2 agents.

Acknowledgements

This new discovery did not receive any external funding. The authors gratefully thank and deeply acknowledge anyone who helped to make this new discovery and work coming out to light.

Conflict of Interest

The authors declare no conflicts of interest.

Data Availability Statement

The data that support the findings of this study are available from the corresponding author upon reasonable request.

Keywords: Anti-COVID-19 drug · 3′-to-5′ Exoribonuclease (ExoN) · Nucleoside analog (NA) · RNA-dependent RNA polymerase (RdRp) · SARS-CoV-2 inhibitor

[1] V. C. Chitalia, A. H. Munawar, *J. Transl. Med.* **2020**, *18*, 390.
[2] X. Wang, R. Cao, H. Zhang, J. Liu, M. Xu, H. Hu, Y. Li, L. Zhao, W. Li, X. Sun, X. Yang, Z. Shi, F. Deng, Z. Hu, W. Zhong, M. Wang, *Cell Discovery* **2020**, *6*, 28.
[3] H. Kaur, P. Sarma, A. Bhattacharyya, S. Sharma, N. Chhimpa, M. Prajapat, A. Prakash, S. Kumar, A. Singh, R. Singh, P. Avti, P. Thota, B. Medhi, *Eur. J. Pharmacol.* **2021**, *906*, 174233.
[4] A. M. Rabie, *Curr. Res. Pharmacol. Drug Discovery* **2021**, *2*, 100055.
[5] A. M. Rabie, *Int. Immunopharmacol.* **2021**, *98*, 107831.
[6] A. Ip, J. Ahn, Y. Zhou, A. H. Goy, E. Hansen, A. L. Pecora, B. A. Sinclaire, U. Bednarz, M. Marafelias, I. S. Sawczuk, J. P. Underwood III, D. M. Walker, R. Prasad, R. L. Sweeney, M. G. Ponce, S. La Capra, F. J. Cunningham, A. G. Calise, B. L. Pulver, D. Ruocco, G. E. Mojares, M. P. Eagan, K. L. Ziontz, P. Mastrokyriakos, S. L. Goldberg, *BMC Infect. Dis.* **2021**, *21*, 72.
[7] J.-C. Tardif, N. Bouabdallaoui, P. L. L'Allier, D. Gaudet, B. Shah, M. H. Pillinger, J. Lopez-Sendon, P. Da Luz, L. Verret, S. Audet, J. Dupuis, A. Denault, M. Pelletier, P. A. Tessier, S. Samson, D. Fortin, J.-D. Tardif, D. Busseuil, E. Goulet, C. Lacoste, A. Dubois, A. Y. Joshi, D. D. Waters, P. Hsue, N. E. Lepor, F. Lesage, N. Sainturet, E. Roy-Clavel, Z. Bassevitch, A. Orfanos, G. Stamatescu, J. C. Grégoire, L. Busque, C. Lavallée, P.-O. Hétu, J.-S. Paquette, S. G. Deftereos, S. Levesque, M. Cossette, A. Nozza, M. Chabot-Blanchet, M.-P. Dubé, M.-C. Guertin, G. Boivin, *Lancet Respir. Med.* **2021**, *9*, 924–932.
[8] E. Mahase, *BMJ* **2021**, *375*, n2713.
[9] M. Imran, M. Kumar Arora, S. M. B. Asdaq, S. A. Khan, S. I. Alaqel, M. K. Alshammari, M. M. Alshehri, A. S. Alshrari, A. Mateq Ali, A. M. Al-shammeri, B. D. Alhazmi, A. A. Harshan, M. T. Alam, Abida, *Molecules* **2021**, *26*, 5795.
[10] D. S. Moirangthem, L. Surbala, *Curr. Drug Targets* **2021**, *22*, 1346–1356.
[11] V. C. Yan, F. L. Muller, *ACS Med. Chem. Lett.* **2020**, *11*, 1361–1366.
[12] L. Brunotte, S. Zheng, A. Mecate-Zambrano, J. Tang, S. Ludwig, U. Rescher, S. Schloer, *Pharmaceutics* **2021**, *13*, 1400.
[13] A. M. Rabie, *ACS Omega* **2022**, *7*, 2960–2969.
[14] A. M. Rabie, *ACS Omega* **2022**, *7*, 21385–21396.
[15] Q. Cai, M. Yang, D. Liu, J. Chen, D. Shu, J. Xia, X. Liao, Y. Gu, Q. Cai, Y. Yang, C. Shen, X. Li, L. Peng, D. Huang, J. Zhang, S. Zhang, F. Wang, J. Liu, L. Chen, S. Chen, Z. Wang, Z. Zhang, R. Cao, W. Zhong, Y. Liu, L. Liu, *Engineering* **2020**, *6*, 1192–1198.
[16] A. M. Rabie, *New J. Chem.* **2021**, *45*, 761–771.
[17] A. M. Rabie, *Mol. Diversity* **2021**, *25*, 1839–1854.
[18] A. M. Rabie, *Chem.-Biol. Interact.* **2021**, *343*, 109480.
[19] A. M. Rabie, *J. Mol. Struct.* **2021**, *1246*, 131106.
[20] M. Chien, T. K. Anderson, S. Jockusch, C. Tao, X. Li, S. Kumar, J. J. Russo, R. N. Kirchdoerfer, J. Ju, *J. Proteome Res.* **2020**, *19*, 4690–4697.
[21] https://www.who.int/en/activities/tracking-SARS-CoV-2-variants (last accessed September 11, 2022).
[22] https://www.washingtonpost.com/health/2021/12/16/omicron-variant-mutations-covid (last accessed September 11, 2022).
[23] S. Khater, P. Kumar, N. Dasgupta, G. Das, S. Ray, A. Prakash, *Front. Microbiol.* **2021**, *12*, 647693.
[24] J. Zhao, Q. Liu, D. Yi, Q. Li, S. Guo, L. Ma, Y. Zhang, D. Dong, F. Guo, Z. Liu, T. Wei, X. Li, S. Cen, *Antiviral Res.* **2022**, *198*, 105254.
[25] J. Zhao, S. Guo, D. Yi, Q. Li, L. Ma, Y. Zhang, J. Wang, X. Li, F. Guo, R. Lin, C. Liang, Z. Liu, S. Cen, *Antiviral Res.* **2021**, *190*, 105078.
[26] X. Lin, C. Liang, L. Zou, Y. Yin, J. Wang, D. Chen, W. Lan, *Eur. J. Med. Chem.* **2021**, *214*, 113233.
[27] I. H. Eissa, M. M. Khalifa, E. B. Elkaeed, E. E. Hafez, A. A. Alsfouk, A. M. Metwaly, *Molecules* **2021**, *26*, 6151.
[28] Y. Wang, L. Chen, *Eur. J. Pharmacol.* **2020**, *889*, 173634.
[29] P. K. Doharey, V. Singh, M. R. Gedda, A. K. Sahoo, P. K. Varadwaj, B. Sharma, *J. Biomol. Struct. Dyn.* **2022**, *40*, 5588–5605.
[30] RdRp. Available from DrugDevCovid19, http://clab.labshare.cn/covid/php/database_target.php?target=RdRp&id=P0DTD1 (last accessed September 9, 2022).
[31] N. H. Moeller, K. Shi, Ö. Demir, C. Belica, S. Banerjee, L. Yin, C. Durfee, R. E. Amaro, H. Aihara, *Proc. Natl. Acad. Sci. USA* **2022**, *119*, e2106379119.
[32] Nsp14. Available from DrugDevCovid19, http://clab.labshare.cn/covid/php/database_target.php?target=nsp14&id=P0DTD1 (last accessed September 10, 2022).
[33] E. C. Smith, H. Blanc, M. C. Surdel, M. Vignuzzi, M. R. Denison, *PLoS Pathog.* **2013**, *9*, e1003565.
[34] F. Ferron, L. Subissi, A. T. Silveira De Morais, N. Le, M. Sevajol, L. Gluais, E. Decroly, C. Vonrhein, G. Bricogne, B. Canard, I. Imbert, *Proc. Natl. Acad. Sci. USA* **2018**, *115*, E162–E171.
[35] H. S. Hillen, G. Kokic, L. Farnung, C. Dienemann, D. Tegunov, P. Cramer, *Nature* **2020**, *584*, 154–156.
[36] S. Jockusch, C. Tao, X. Li, T. K. Anderson, M. Chien, S. Kumar, J. J. Russo, R. N. Kirchdoerfer, J. Ju, *Antiviral Res.* **2020**, *180*, 104857.
[37] Riboprine. PubChem CID: 24405. Available from PubChem, https://pubchem.ncbi.nlm.nih.gov/compound/Riboprine (last accessed September 11, 2022).
[38] G. A. Kicska, L. Long, H. Hörig, C. Fairchild, P. C. Tyler, R. H. Furneaux, V. L. Schramm, H. L. Kaufman, *Proc. Natl. Acad. Sci. USA* **2001**, *98*, 4593–4598.
[39] A. M. Rabie, M. Abdalla, *Med. Chem. Res.* **2023**, *32*, In Press. https://doi.org/10.1007/s00044-022-02970-3.
[40] M. Abdalla, A. M. Rabie, *Comput. Biol. Chem.* **2023**, *102*, 107768. https://doi.org/10.1016/j.compbiolchem.2022.107768.

Submitted: May 16, 2022
Accepted: September 30, 2022